Verification-based Safe Policy Synthesis

Anonymous Author(s)

Abstract

We present Marvel, a verification-based control policy synthesis framework to address safe reinforcement learning in continuous state and action space. The key idea is the integration of program reasoning techniques into reinforcement learning training loops. Marvel performs abstraction based program verification to reason about a policy and its environment as a closed-loop system. Based on a novel counterexample guided inductive synthesis loop for training, Marvel reduces the amount of safety violation in the system abstraction, which approximates the safety loss of the *worst-case* inputs, using gradient-descent style optimization. When an environment is unknown or its complexity does not allow scalable verification, Marvel accurately approximates it with a lightweight model to support efficient verification. Experimental results of a wide range of applications including the challenging Mujoco environments demonstrate the substantial benefits of leveraging verification feedback for control policy safe-by-construction.

1 Introduction

Policy search is commonly used to govern cyber-physical systems such as autonomous vehicles, where high assurance is particularly important. Reinforcement Learning (RL) is a promising approach for policy search [16]. State-of-the-art RL algorithms can learn motor skills autonomously through trial and error in simulated or even unknown environments, thus avoiding tedious manual engineering. However, the most performant policies may still be unsafe since the RL algorithms do not provide any formal guarantees on safety. A learned policy may fail occasionally but catastrophically, and debugging these failures can be challenging [43]. For example, a self-driving car navigates to a target region, while avoiding a trap zone, may still enter unsafe corner regions irregularly after training.

Guaranteeing the safety of a reinforcement learning policy is therefore important. Since a control policy is just a program, principally it can be verified or even synthesized using program verification and program synthesis. Indeed, the use of automated program reasoning techniques to aid the design of reliable machine learning systems has risen rapidly over the last few years. A notable example is the application of abstract interpretation [12] to verify robustness of convolutional neural networks [18]. For supervised learning, the robustness property of a neural network requires that its outputs be consistent for narrow input spaces surrounding individual data points. A natural extended question is that can we use program verification and synthesis to address safe reinforcement learning where a system includes both an environment and a policy? Moreover, in case verification fails, can we exploit verification counterexamples to synthesize a safe policy? These are challenging problems because safety properties must be enforced in a much wider space including all possible initial states of the system.

For reinforcement learning in an unknown environment, the primary barrier of safety verification is that we have no clue about the state transition probability distribution of the environment. The absence of environment models prevents verifying an environment and a learned policy as a combined closed-loop system. Even in a simulated environment with a known state transition model, safety verification is still challenging because the model typically involves complex nonlinear behaviors that are difficult to estimate or characterize. State space over-approximation may quickly incur large error which results in abstraction that is too conservative and cannot be used for safety verification [14, 15, 41]. When verification fails, these approaches provide little insight on how to effectively leverage counterexamples to improve safety. To address the large approximation error, one could use statistical model checking to sample rollouts and evaluate the safety property with statistical confidence [50]. The question remains of how the verification results might help further optimize the policy if the confidence level is not desirable.

To overcome these difficulties, we present Marvel as a new verification-based policy synthesis framework, depicted in Fig. 1. It consists of three main components, namely *environment model inference*, *policy verification*, and *policy synthesis*.

- **Environment Model Inference**. For an unknown environment or a simulated environment whose state transition model is, however, out of the reach of state-of-the-art verification techniques, Marvel accurately approximates the environment using a lightweight *time-varying linear Gaussian* state transition model, which is tractable for both learning and verification. Note that this component is optional since Marvel supports safety verification based on user-provided nonlinear environment models [4] as well.
- **Policy Verification**. Given an environment model and a policy, Marvel verifies the model and the policy as a combined closed-loop system using abstract interpretation.
- **Policy Synthesis**. A safety counterexample detected by Marvel is a *symbolic rollout* of abstract states of the closed-loop system because it is obtained by abstract interpretation. Marvel quantifies the violation of safety properties by the abstract states. The goal of policy synthesis is to effectively reduce the amount of safety violation to zero.

PL'18, January 01–03, 2018, New York, NY, USA
2018.

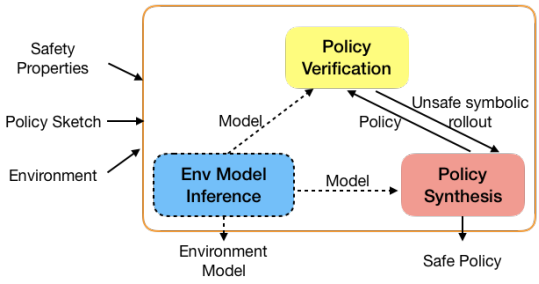

Figure 1. Our policy synthesis framework **Marvel**: **M**odel-**A**ided **R**easoning for **V**erification-**E**nabled **L**earning

Based on this discussion, the main technical contributions of this paper are twofold: First, in case when environments are unknown or their complexity does not allow scalable verification, we introduce a model-based approach that builds an environment model from observations that is useful for efficient policy verification. Marvel verifies a policy with respect to the environment model, which can be used to generate synthetic but tight abstraction of actual system behaviors. With a high-accuracy model, formal guarantees based on the learned model can be generalized to real experience with high probability. The model itself is valuable as it pinpoints part of the state space where the policy is trustworthy.

Second, the policy synthesis procedure is designed with formal verification in mind and is realized through a novel counterexample guided inductive synthesis (CEGIS) [38] loop. The most important feature of our CEGIS is that, instead of synthesizing a policy with *concrete* examples, we use *symbolic rollouts* with abstract states obtained by abstract interpretation. Marvel reduces the amount of safety properties violation by the abstraction states, which approximates the safety loss by the *worst-case* input, using a lightweight gradient-descent style optimization. Thus, Marvel can efficiently leverage verification feedback in a learning loop to enable policy safe-by-construction.

We present a detailed experimental study over a wide range of reinforcement learning systems. Our results manifest that Marvel can accurately approximate unknown environments or environments with complex dynamics using a lightweight model that facilitates scalable policy verification. Our experiments demonstrate the benefits of integrating formal verification as part of the training objective and leveraging verification feedback for safe policy synthesis.

Contributions. To summarize, this paper makes the following contributions:

- We propose a new model-based framework for safe policy synthesis for challenging or even unknown environments.
- We present an efficient approach to allow the use of verification in a training loop for policy safe-by-construction.
- We implement the proposed ideas in a tool called Marvel and evaluate it in various application domains, proving that verification-based safe policy synthesis is achievable even for high-dimensional systems.

2 Motivation and Overview

To motivate the problem and to provide an overview of our approach, consider the CartPole environment taken from OpenAI Gym [10]. A pictorial view of the environment is given below. A pole is attached by an unactuated joint to a cart, which moves along a frictionless track. The pendulum starts close upright, and the goal is to prevent it from falling over more than 12 degrees from vertical or moving more than 2.4 units from the center. A control policy can do so by taking actions to increase or reduce the cart's velocity. To make the example more interesting and challenging, (1) we strengthened the safety constraint: the cart is not allowed to move more than 0.5 units from the center (2) a policy for the CartPole environment applies a continuous action as opposed to a discrete force to control the system. A system as such is representative of a number of practical Markov Decision Processes (MDPs), such as autonomous drones, that have thus far proven difficult for safety verification, but for which high assurance is extremely important.

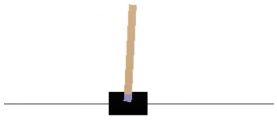

For the CartPole problem, even if the environment model is explicitly provided[1], safety verification is still infeasible as the model's state transition function involves complex system dynamics and nonlinear computations which are out of the reach of state-of-the-art verification techniques. We now explain our key ideas using the CartPole environment.

2.1 Safety Specification

According to the OpenAI Gym test criteria, the CartPole problem is considered solved when the learned policy can balance the pole well, while ensuring the cart not moving out of the safety range, within 200 timesteps over 100 consecutive rollouts. We specify the safety property formally. The CartPole problem is modeled as an MDP (**Sec. 3**) of four variables $x, \dot{x}, \theta, \dot{\theta}$, representing cart position, velocity, pole angle, and angular velocity. According to the test criteria, we specify the initial states S_0 as

$$S_0 \equiv \{(x, \dot{x}, \theta, \dot{\theta}) \mid -0.05 \leq x, \dot{x}, \theta, \dot{\theta} \leq 0.05\}$$

The safety property φ_{safe} of the system is specified as

$$\varphi_{safe}((x, \dot{x}, \theta, \dot{\theta})) \equiv -0.5 \leq x \leq 0.5 \wedge -0.21 \leq \theta \leq 0.21$$

(12 degrees $\approx$ 0.21 radians). Given the time horizon $T = 200$ timesteps, a safe policy for the CartPole problem aims to ensure that, for any state s in a T-step episode rollout from an initial state in S_0, $\varphi_{safe}(s)$ is true.

[1] https://gym.openai.com/envs/CartPole-v1/

However, φ_{safe} is a weak safety property. For various policies trained by reinforcement learning algorithms [27, 33, 35] in the CartPole environment, even though they can pass the test criteria, we observed that sometimes the RL agents tend to lose balance approaching 200 timesteps. We also lack a formal guarantee that the policy works well for unsampled rollouts. Our goal is to learn a policy that can be shown safe in *infinite timesteps* for *all possible initial states*. To this end, we introduce another safety property φ_{reach}, requiring that certain goal condition be met eventually. For the CartPole problem, we set φ_{reach} *equivalent to the specification of the initial states*:

$$\varphi_{reach}((x, \dot{x}, \theta, \dot{\theta})) \equiv -0.05 \leq x, \dot{x}, \theta, \dot{\theta} \leq 0.05$$

We define that a CartPole episode rollout from an initial state s_0 is *safe* iff there exists $T' \leq T$ ($T = 200$) such that:

$$\underbrace{s_0}_{\varphi_{reach}(s_0)}, \quad \underbrace{s_1, \ldots, s_{T'-1}}_{\forall i \in 1 \ldots T'-1,\ \varphi_{safe}(s_i)} \quad \underbrace{s_{T'}}_{\varphi_{reach}(s_{T'})} \tag{1}$$

Essentially, we specified φ_{reach} as an *inductive invariant* of the CartPole problem: (1) φ_{reach} is equivalent to the initial state set, (2) any rollout starting from φ_{reach} eventually turns back to it, (3) any states in a rollout (including those that temporarily leave the inductive invariant set) are safe.

2.2 Environment Model Inference

As discussed above, verifying a CartPole policy against the safety property φ_{safe} and the inductive invariant φ_{reach} is challenging. Our solution is based on model-based learning, which samples and learns the probabilistic state transition model and uses it to verify the policy and improve the policy based on the verification feedback in a learning loop.

It is well-known that physical systems such as robots, including the CartPole problem, can be reasonably approximated by piecewise linear dynamics. We learn the model of a physical system as *time-varying linear-Gaussian* (TVLG) [25], a kind of piecewise linear models. The state transition of TVLG at each timestep depends on a *Gaussian* distribution:

$$s_{t+1} \sim \mathcal{N}(A_t \cdot s_t + B_t \cdot a_t + c_t, \Sigma_t)$$

where s_{t+1} (resp. s_t) is a sampled state at timestep $t+1$ (resp. t) and a_t is an action taken at t. The mean of the Gaussian distribution is *linear* to s_t and a_t weighted by A_t and B_t (added with a bias vector c_t). State transition is *time-varying* as A_t, B_t, c_t, and covariance Σ_t vary at each timestep, allowing the model to capture highly non-linear transition functions[2]. For action planning in the CartPole environment, we consider a linear-Gaussian state feedback policy:

$$a_t \sim \pi(\cdot \mid s_t) = \mathcal{N}(K \cdot s_t + k, S)$$

[2]Although stochastic dynamics could possibly violate the local linearity assumption, in practice, this representation was found well suited for modeling various noisy real-world tasks [25].

The policy π generates an action a_t that is *linear* to states s_t weighted by policy parameters K and k, and affected by a diagonal covariance matrix S (which is state-independent).

The main reason that we use time-vary linear-Gaussian to approximate highly-nonlinear or unknown environments is that such a model is tractable for both *learning* and *verification*. For learning, the particular form of a TVLG model implies that one can simply use linear regression to determine A_t, B_t, c_t, and then fit Σ_t based on the errors at each timestep t for the CartPole problem with rollouts sampled from the OpenAI Gym environment, using the current policy $\pi(a_t|s_t)$. The challenge is that the sample complexity of linear regression scales with the dimensionality of states. For a much higher-dimensional robotic system than CartPole, the need of large number of samples to obtain a good dynamics fit at each timestep can be reduced by bringing in information from a global model fitted to all of the transitions from other time steps (**Section. 4.2.1**), or even prior models [25].

2.3 Policy Verification

Since both the CartPole environment model and the policy are linear-Gaussian, the combined MDP system of the model and the policy is still linear-Gaussian. This is because the sum of Gaussian variables is again a Gaussian variable. From an initial state, (*i*) the mean μ_{s_t} of all possible states sampled at a timestep t can be computed by a *linear* system whose state-transition model is linear to the dynamics matrices A_t, B_t, c_t, and policy parameters K and k:

$$\begin{aligned} \mu_{a_t} &= K \cdot \mu_{s_t} + k, && \forall t \geq 0 \\ \mu_{s_{t+1}} &= A_t \cdot \mu_{s_t} + B_t \cdot \mu_{a_t} + c_t, && \forall t \geq 0 \end{aligned} \tag{2}$$

(*ii*) the deviations of all possible states from the mean at t are constrained by the *Gaussian* covariances $\Sigma_1, \ldots, \Sigma_t$ (**Sec. 4.2**). We exploit the two nice features (*i*) and (*ii*) to build a TVLG verification procedure based on *abstract interpretation*.

At each timestep t, a tight abstraction of the *linear* system in equation (2) combined with a box estimation of the standard *Gaussian* deviations in the covariance matrix (under a chosen probabilistic coverage) can accurately approximate possible states that can be sampled from a TVLG model at t (**Sec. 4.2.2**). With an abstract domain, the computation of the abstract semantics of TVLG yields a *symbolic rollout* of abstract states. We use the DeepPoly abstract domain [37] for this example. An abstract state in the DeepPoly domain is a tuple $\langle a^{\leq}(X), a^{\geq}(X), l, u \rangle$ where $a^{\leq}$ and $a^{\geq}$ are the (symbolic) lower and upper polyhedral constraints over the system variables X. l and u are the concrete lower and upper bounds that over-approximate the two symbolic bounds. One simple concertization of the abstract state is the interval (l, u) as it gives the state value upper- and lower-bounds.

We depict the interval concretization of each abstract state within the symbolic rollout of a TVLG-approximated CartPole system in Fig. 2a in red and we only show the abstraction for cart positions x. It can be seen that all states within the

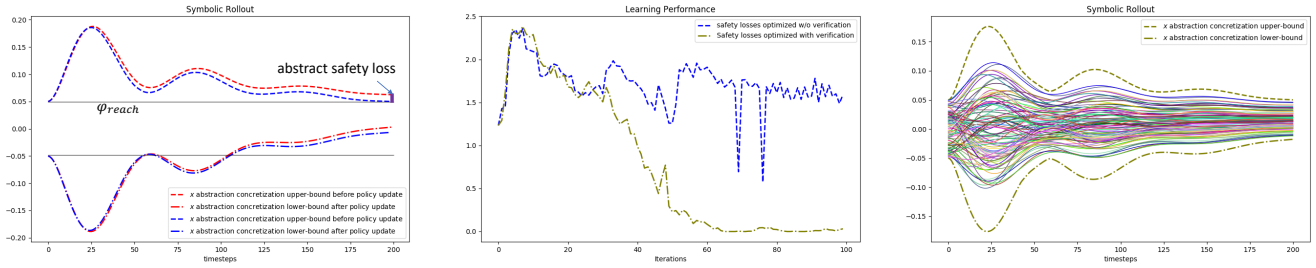

(a) Verification-based Policy Update **(b)** Marvel and NG-LIN Safety losses **(c)** Environment Model Accuracy

Figure 2. Verification-based policy update (a), Learning performance (b), and model accuracy (c) of the CartPole Problem

upper- and lower-bounds satisfy φ_{safe}. However, φ_{reach} is not satisfied as the upper bounds of cart positions are above 0.05, which is informally the upper-bound of cart position in φ_{reach}. Clearly, φ_{reach} is not an inductive invariant as per equation (1) for the trained system because there is a gap between the red upper-bound and that of φ_{reach} at the last timestep, which we refer to as *abstract safety loss*. The loss is computed based on abstraction. As depicted in Fig. 2a, the abstract safety loss approximates the safety loss of the *worst-case* input. We formally characterize the abstract safety loss between abstract states and safety properties in **Sec. 4.2.3**.

A simple verification strategy is to iteratively run abstract interpretation to verify the learned policies at each RL iteration with a fitted TVLG model of the environment. The algorithm terminates when a safe policy is found. However, the simple strategy does not work as shown in Fig. 2b. The blue curve records the abstract safety losses of the RL policies learned by an RL algorithm NG-LIN [33] at each training iteration. We choose this algorithm because it performed better than other RL algorithms for this environment, e.g. [29, 35]. A previous TVLG-model-based RL algorithm [25] also fails this task. This result is not very surprising as the RL algorithms do not attempt to use verification feedback for safety improvement. Although they can learn high-reward policies, there is no safety guarantee provided by these algorithms.

2.4 Policy synthesis

One unique feature of our safe policy synthesis algorithm is that it consists in a symbolic counterexample guided inductive synthesis (**CEGIS**) loop. When verification fails we use symbolic rollouts as counterexamples to improve policy safety. In Fig. 2a, the abstract safety loss of the red unsafe symbolic rollout is based on an abstract state. Abstract states are nonetheless parameterized by policy parameters (K, k and S) as shown in equation (2). Thus, we can leverage a gradient-descent style optimization to update policy parameters by taking steps proportional to the negative of the gradient of the abstract safety loss. As opposed to standard gradient descent, our CEGIS algorithm optimizes policies based on symbolic rollouts in an abstract domain, favouring the safety verifier directly for provable guarantees. Fig. 2a depicts the symbolic rollout of the updated policy in blue where the abstract safety loss is reduced.

The primary challenge for model-based policy updates is that a fitted TVLG model is only locally correct in a region of the state space around the sampled rollouts driven by the old policy. An unconstrained policy update may cause the new policy to fall into part of the state space where the TVLG model is incorrect, preventing convergence. However, too conservative policy updates may slow down learning. Moreover, such updates do not incorporate reward signals which may include performance constraints other than safety. We address these problems by formalizing a new safe policy synthesis algorithm that (1) provides verification-based policy gradients along the most promising direction to enhance both safety and reward performance and (2) improves the policy even in situations where we have to trade off model consistency for a relatively large policy update (**Sec. 4.2.4**).

Fig. 2b compares the performance of our approach and NG-LIN for the CartPole problem. Our algorithm discovered a verified policy with zero abstract safety loss at 65 iteration (olive curve) while the RL algorithm struggled to find a safe policy (blue curve). The result demonstrates that optimizing policies with the safety verifier providing policy gradients directly in the proof space outperforms policy updates solely using simulated rollouts.

To show the accuracy of the fitted TVLG model for the CartPole problem, we simulated a learned safe policy in the environment. A model is *accurate* if the simulated rollouts lie within the interval conretization of abstract states within the system's symbolic rollout. As depicted in Fig. 2c, the learned model is accurate for cart position x. It is accurate for the other dimensions as well (see the Appendix. A.1).

3 Problem Setup

We formulate safe policy synthesis in the context of Markov Decision Process with probabilistic dynamics.

MDP. Formally, an MDP is a structure $M = (X, S, A, F : \{S \times A \to S\}, S_0, \varphi_{safe}, \varphi_{reach}, R : \{S \times A \to \mathbb{R}\}, \beta)$ where X is a finite set of variables interpreted over the reals $\mathbb{R}$; S is

an infinite set of *continuous real-vector* environment states which are valuations of the variables X ($S \subseteq \mathbb{R}^{|X|}$); A is a set of *continuous real-vector* agent actions; F is a stochastic state transition function that emits the next environment state given a current state s and an agent action a; $F(s,a)$ is defined as some probabilistic distribution $P(\cdot|s,a)$; we assume that the initial states of M are uniformly sampled from a set of environment states $S_0 \subseteq S$. $R(s,a)$ is the immediate reward after transition from an environment state s with action a and $0 < \beta \leq 1$ is a reward discount factor.

Policy. An agent of an MDP M can interact with the environment by taking actions via a policy conditioned on environment states. Formally, a policy is a (stochastic) map $\pi : \{S \rightarrow A\}$ that determines which action the agent ought to take in a given state. Popular policy structures include neural networks and linear functions.

MDP Rollout. Given a time horizon T, a T-timestep MDP rollout is $s_0, a_0, s_1, \ldots, s_{T'}$ where $T' \leq T$ and s_t and a_t are the environment state and the action taken at timestep t such that $s_0 \in S_0$, $s_{t+1} \sim F(s_t, a_t)$, and $a_t \sim \pi(a_t|s_t)$. The aggregate reward of a policy π is

$$J(\pi) = \mathbb{E}_{s_0,a_0,\ldots}[\Sigma_i \beta^i R(s_i, a_i)]$$

Policy search, such as reinforcement learning, aims to produce a policy π that maximizes $J(\pi)$.

Safe MDP Rollout. In this work, an MDP M includes two safety properties φ_{safe} and φ_{reach} as logical formulae over environment states. They specify the intended behavior of any agents of M. φ_{safe} enforces that agents should only visit safe environment states evaluated true by φ_{safe}. For example, an agent should remain within a safety boundary or avoid any obstacles. Additionally, M enforces that agents should eventually reach some environment states evaluated true by φ_{reach}. For instance, an agent should meet some goals.

Definition 3.1 (Safety Property)**.** Given an MDP, S_0 defines a bounded domain in the form of an interval $[\underline{x}, \overline{x}]$ where $\underline{x}, \overline{x} \in \mathbb{R}^{|X|}$ are lower and upper bounds of the initial states. Both φ_{safe} and φ_{reach} are quantifier-free Boolean combinations of linear inequalities over the MDP's variables X:

$\langle \varphi_{safe},\ \varphi_{reach} \rangle ::= \langle P \rangle \mid \langle P \rangle \wedge \langle P \rangle \mid \langle P \rangle \vee \langle P \rangle$;

$\langle P \rangle ::= \mathcal{A} \cdot x \leq b$ *where* $\mathcal{A} \in \mathbb{R}^{|X|}$, $b \in \mathbb{R}$;

An MDP state $s \in S$ satisfies φ_{safe} or φ_{reach}, denoted as $s \models \varphi_{safe}$ or $s \models \varphi_{reach}$, iff $\varphi_{safe}(s)$ or $\varphi_{reach}(s)$ is true.

A T-timstep MDP rollout $s_0, a_0, s_1, \ldots, s_{T'}$ ($T' \leq T$) is *safe* with respect to φ_{safe} and φ_{reach} iff:

$$\underbrace{s_0, a_0, s_1, \ldots a_{T'-2}, s_{T'-1}}_{\forall i \in 1 \ldots T'-1,\ s_i \models \varphi_{safe}} \underbrace{a_{T'-1}, s_{T'}}_{s_{T'} \models \varphi_{reach}}.$$

We require that the reward function R of an MDP be consistent with φ_{safe} and φ_{reach}. In fact, one can use reward shaping to design reward signals encouraging a policy to satisfy φ_{safe} and φ_{reach} by learning.

Safe Policy. Other than maximizing the accumulative reward $J(\pi)$, we aim to develop safe policy synthesis producing MDP policies that can be formally verified safe. Given an MDP M and a time horizon T, a policy π is *safe*, denoted as $M[\pi] \models \varphi_{safe}, \varphi_{reach}$, iff any T-timestep rollout of M is safe.

4 Verifiable Safe policy synthesis

We firstly focus on safe policy synthesis for a kind of MDPs with a *known* and *deterministic* state transition dynamics function in Sec. 4.1. In this case, at each timestep t, an MDP's state transition function $F(s_t, a_t)$ produces a deterministic next state s_{t+1}. We defer safe policy synthesis for general stochastic environments with unknown state transition dynamics to Sec. 4.2, which further extends our solution for the deterministic case in Sec. 4.1.

4.1 Safe policy synthesis for Deterministic Models

Given an MDP M with deterministic dynamics, it suffices to learn a deterministic policy $a_t = \pi(s_t)$ to control M.

Definition 4.1 (**DSTS** – Deterministic State Transition Systems)**.** For an MDP $M = (X, S, A, F, S_0, \varphi_{safe}, \varphi_{reach}, R, \beta)$, if the state transition function $F : \{S \times A \rightarrow S\}$ is deterministic, M can be redefined as a deterministic state transition system $\mathcal{F}[\cdot] = (F,\ \cdot,\ S_0)$, parameterized by an unknown deterministic policy $\pi : S \rightarrow A$, where the state transition function F receives control actions given by the policy and S_0 is the initial state space. We explicitly model policy deployment as $\mathcal{F}[\pi] = (F, \pi, S_0)$. Structurally, $\mathcal{F}[\pi]$ consists of T layers. Each layer at t ($t \geq 0$) is a function F_π^t: $\lambda s_t.F(s_t, \pi(s_t))$, which takes as input a state s_t at timestep t and outputs its next state s_{t+1} at timestep $t+1$. Formally, layer t is a compositional function of an initial state: $\mathcal{F}_t[\pi] = F_\pi^{t-1} \circ \ldots \circ F_\pi^1 \circ F_\pi^0$.

Similar to the general MDP case, given a time horizon T, a deterministic policy π is safe for a deterministic state transition system $\mathcal{F}[\cdot]$ with respect to φ_{safe} and φ_{reach}, denoted as $\mathcal{F}[\pi] \models \varphi_{safe}, \varphi_{reach}$, iff, for any rollout of $\mathcal{F}[\pi]$,

$$\underbrace{s_0, s_1, \ldots s_{T'-2}, s_{T'-1}}_{\forall t \in 1 \ldots T'-1,\ s_i \models \varphi_{safe}} \underbrace{s_{T'}}_{s_{T'} \models \varphi_{reach}}$$

where $T' \leq T$, $s_0 \in S_0$ and $\forall t \geq 0, s_{t+1} = \mathcal{F}_t[\pi](s_0)$.

4.1.1 DSTS Policy Verification.

To verify a DSTS over an infinite set of initial states, we apply abstract interpretation to approximate the infinite set of system behaviors.

Abstract Interpretation. We verify the safety of a deterministic state transition system (**DSTS**) using abstract interpretation. The abstract interpretation framework [28, 37] is defined as a tuple: $\langle \mathcal{D}_c, \mathcal{D}_a, \alpha, \gamma, f \rangle$ where

- $\mathcal{D}_c : \{s \mid s \in \mathbb{R}^d\}$ is the concrete domain;
- $\mathcal{D}_a$ is the abstract domain of interest;
- $\alpha(\cdot)$ is an *abstraction* function that maps a set of concrete elements to an abstract element;

- $\gamma(\cdot)$ is a *concretization* function that maps an abstract element to a set of concrete elements;
- $f = \{(f_c, f_a) \mid f_c(\cdot) : \mathcal{D}_c \to \mathcal{D}_c, f_a(\cdot) : \mathcal{D}_a \to \mathcal{D}_a\}$ is a set of transformer pairs over $\mathcal{D}_c$ and $\mathcal{D}_a$.

The abstract interpretation framework is sound [37] if for all $S \subseteq \mathcal{D}_c$, $S \subseteq \gamma(\alpha(S))$ holds and given $(f_c, f_a) \in f$,

$$\forall c \in \mathcal{D}_c, a \in \mathcal{D}_a,\ c \in \gamma(a) \implies f_c(c) \in \gamma(f_a(a)).$$

Definition 4.2 (DSTS Abstract Interpretation)**.** Given a deterministic state transition system $\mathcal{F}[\pi] = (F, \pi, S_0)$, let $\mathcal{D} = \langle \mathcal{D}_c \equiv S, \mathcal{D}_a, \alpha, \gamma, f\}\rangle$ be an instantiated abstract interpreter with a chosen abstract domain $\mathcal{D}_a$, abstraction function α, and concretization function γ. For every operation $\iota_c(\cdot)$ in F and π, there exists a suitable abstract transformer ι_a such that $(\iota_c, \iota_a) \in f$.

For a DSTS $\mathcal{F}[\pi]$ and an abstract interpreter $\mathcal{D}$, we denote by $\mathcal{F}_t^{\mathcal{D}}[\pi] : \mathcal{D}_a \to \mathcal{D}_a$ the over-approximation of $\mathcal{F}_t[\pi]$ (Definition 4.1) using $\mathcal{D}$ where any operations $\iota_c(\cdot)$ in $F(\cdot)$ and policy $\pi(\cdot)$ in $\mathcal{F}_t[\pi]$ are replaced in $\mathcal{F}_t^{\mathcal{D}}[\pi]$ by their corresponding abstract transformers ι_a in $\mathcal{D}$.

Definition 4.3 (DSTS Symbolic Rollout)**.** Given a deterministic state transition system $\mathcal{F}[\pi] = (F, \pi, S_0)$ and an abstract interpreter $\mathcal{D}$, a symbolic rollout of $\mathcal{F}$ over $\mathcal{D}$ is $S_0^{\mathcal{D}}, S_1^{\mathcal{D}}, \ldots$ where $S_0^{\mathcal{D}} = \alpha(S_0)$ is the abstraction of the initial states S_0. And $S_t^{\mathcal{D}} = \mathcal{F}_t^{\mathcal{D}}[\pi]\big(\alpha(S_0)\big)$ over-approximates all possible states in the concrete domain corresponding to any initial state $s_0 \in S_0$ at timestep t.

Theorem 4.4 (DSTS Over-approximation Soundness)**.** *For a deterministic state transition system $\mathcal{F}[\pi]$, given an abstract interpreter $\mathcal{D}$, at arbitrary timestep t, we have:*

$$\forall s_0.\ s_0 \in S_0 \implies \mathcal{F}_t[\pi]\ (s_0) \in \gamma\Big(\mathcal{F}_t^{\mathcal{D}}[\pi]\big(\alpha(S_0)\big)\Big).$$

4.1.2 DSTS Policy Safety Loss.

Any unsafe rollouts of a policy must have violated safety properties at some states. We define a safety loss function to quantify the safety violation of a state.

Definition 4.5 (Safety Loss Function)**.** For a safety property φ over states $s \in S$, we define a non-negative loss function $\mathcal{L}(s, \varphi)$ such that $\mathcal{L}(s, \varphi) = 0$ iff s satisfies φ, i.e. $s \models \varphi$. We define $\mathcal{L}(s, \varphi)$ recursively, based on the possible shapes of φ (Definition 3.1):

- $\mathcal{L}(s, \mathcal{A} \cdot x \le b) := \max(\mathcal{A} \cdot s - b, 0)$
- $\mathcal{L}(s, \varphi_1 \wedge \varphi_2) := \max(\mathcal{L}(s, \varphi_1), \mathcal{L}(s, \varphi_2))$
- $\mathcal{L}(s, \varphi_1 \vee \varphi_2) := \min(\mathcal{L}(s, \varphi_1), \mathcal{L}(s, \varphi_2))$

Note that $\mathcal{L}(s, \varphi_1 \wedge \varphi_2) = 0$ iff $\mathcal{L}(s, \varphi_1) = 0$ and $\mathcal{L}(s, \varphi_2) = 0$, which by construction is true if both φ_1 and φ_2 are satisfied by s, and similarly $\mathcal{L}(\varphi_1 \vee \varphi_2) = 0$ iff $\mathcal{L}(\varphi_1) = 0$ or $L(\varphi_2) = 0$.

Although it is possible to learn DSTS policy parameters using the safety loss function as a negative reward function with reinforcement learning, we do not have any formal safety guarantee of a learned policy. Instead, we aim to use verification feedback to improve policy safety. To this end, we lift the safety loss function over concrete states (Definition 4.5) to an *abstract safety loss* function for over-approximated abstract states.

Definition 4.6 (Abstract Safety Loss Function)**.** Given an abstract state $S^{\mathcal{D}}$ and a safety property φ, we define an abstract safety loss function as

$$\mathcal{L}_{\mathcal{D}}(S^{\mathcal{D}}, \varphi) = \max_{s \in \gamma(S^{\mathcal{D}})} \mathcal{L}(s, \varphi)$$

The abstract safety loss function applies γ to obtain all concrete states represented by an abstract state $S^{\mathcal{D}}$. It measures the worst-case safety loss of φ among all concrete states subsumed by $S^{\mathcal{D}}$. Observe that, given an abstract domain $\mathcal{D}_a$, we can usually approximate $\gamma(S^{\mathcal{D}})$ with a tight interval $\gamma_I(S^{\mathcal{D}})$. For example, given $\mathcal{D}_a$ as a zonotope domain, $S^{\mathcal{D}} \equiv \langle z_C, z_E\rangle$ where $z_C \in \mathbb{R}^{|X|}$ is the center of the zonotope, and $z_E \in \mathbb{R}^{|X| \times m}$ for some m describes a linear relationship between the error vector $e \in [-1, 1]^m$ and the output. The approximated interval concretization of $S^{\mathcal{D}}$ is [30]:

$$\gamma_I(S^{\mathcal{D}}) = \big([(z_C)_i - \Sigma_{j=1}^m |(z_E)_{i,j}|]_i, [(z_C)_i + \Sigma_{j=1}^m |(z_E)_{i,j}|]_i\big)$$

Hence, based on the possible shape of φ, we can more efficiently compute $\mathcal{L}_{\mathcal{D}}(S^{\mathcal{D}}, \varphi)$ as:

- $\mathcal{L}_{\mathcal{D}}(S^{\mathcal{D}}, \mathcal{A} \cdot x \le b) := \max_{s \in \gamma_I(S^{\mathcal{D}})} \big(\max(\mathcal{A} \cdot s - b, 0)\big)$
- $\mathcal{L}_{\mathcal{D}}(S^{\mathcal{D}}, \varphi_1 \wedge \varphi_2) := \max(\mathcal{L}_{\mathcal{D}}(S^{\mathcal{D}}, \varphi_1), \mathcal{L}_{\mathcal{D}}(S^{\mathcal{D}}, \varphi_2))$
- $\mathcal{L}_{\mathcal{D}}(S^{\mathcal{D}}, \varphi_1 \vee \varphi_2) := \min(\mathcal{L}_{\mathcal{D}}(S^{\mathcal{D}}, \varphi_1), \mathcal{L}_{\mathcal{D}}(S^{\mathcal{D}}, \varphi_2))$

Theorem 4.7 (Abstract Safety Loss Function Soundness)**.** *Given an abstract state $S^{\mathcal{D}}$ and a safety property φ, we have:*

$$\mathcal{L}_{\mathcal{D}}(S^{\mathcal{D}}, \varphi) = 0 \implies s \models \varphi\ \forall s \in \gamma_I(S^{\mathcal{D}}).$$

We further extend the definition for the safety of an abstract state to the safety of a symbolic rollout.

Definition 4.8 (Symbolic Rollout Safety Loss)**.** Given a DSTS $\mathcal{F}[\pi]$, its T-step symbolic rollout $S_0^{\mathcal{D}}, S_1^{\mathcal{D}}, S_2^{\mathcal{D}}, \ldots, S_{T-1}^{\mathcal{D}}, S_T^{\mathcal{D}}$ (Definition 4.3) satisfies the safety properties φ_{safe} and φ_{reach} iff there exists $T' \le T$ such that:

$$\underbrace{S_0^{\mathcal{D}}, S_1^{\mathcal{D}}, S_2^{\mathcal{D}}, \ldots, S_{T'-1}^{\mathcal{D}}}_{\forall t \in 1 \ldots T'-1,\ \mathcal{L}_{\mathcal{D}}(S_t^{\mathcal{D}}, \varphi_{safe}) = 0} \qquad \underbrace{S_{T'}^{\mathcal{D}}}_{\mathcal{L}_{\mathcal{D}}(S_{T'}^{\mathcal{D}}, \varphi_{reach}) = 0}$$

If the symbolic rollout is unsafe, the safety loss of $\mathcal{F}[\pi]$ is:

$$\mathcal{L}_{\mathcal{D}}(\mathcal{F}[\pi], \varphi_{safe}, \varphi_{reach}) = \mathcal{L}_{\mathcal{D}}(S_T^{\mathcal{D}}, \varphi_{reach}) + \Sigma_{t=1}^T \mathcal{L}_{\mathcal{D}}(S_t^{\mathcal{D}}, \varphi_{safe})$$

Given a DTST system $\mathcal{F}[\pi] = (F, \pi, S_0)$, if the deployed policy π is complex (e.g. neural networks) or the state transition function F is nonlinear, abstract interpretation over the entire initial state space S_0 could incur very coarse abstractions, thereby giving false alarms. Initial state space partitioning is a common strategy to defeat large approximation error. Using a similar strategy to [46], we pick state dimensions that significantly contribute to the unsafety of the $\mathcal{F}[\pi]$ symbolic rollout (Definition 4.8) based on their

cumulative gradient of the abstract safety loss function (by calculation or estimation see below). A larger gradient suggests greater potential of decreasing the abstract safety loss if we bisect the initial state space along the picked dimensions. Formally, an input space partition of $\mathcal{F}$ is $\mathcal{F}^1, \mathcal{F}^2, \ldots, \mathcal{F}^N$ where $\mathcal{F}^i[\pi] = (F, \pi, S_0^i)$ and $S_0 = \bigcup_{i=1}^N S_0^i$. The safety loss of $\mathcal{F}$ can be redefined as:

$$\mathcal{L}_{\mathcal{D}}(\mathcal{F}[\pi], \varphi_{safe}, \varphi_{reach}) = \frac{1}{N}\sum_{i=1}^{N} \mathcal{L}_{\mathcal{D}}(\mathcal{F}^i[\pi], \varphi_{safe}, \varphi_{reach})$$

The above and Definition 4.8 specifies a sound verification procedure for DSTS, formalized below.

Theorem 4.9 (Safety Verification Soundness)**.** *For a DTST system $\mathcal{F}[\pi]$ deployed with a deterministic policy π, $\mathcal{F}[\pi] \models \varphi_{safe}, \varphi_{reach}$ denotes that the deployed system satisfies safety properties φ_{safe} and φ_{reach}.*

$$\mathcal{L}_{\mathcal{D}}(\mathcal{F}[\pi], \varphi_{safe}, \varphi_{reach}) = 0 \implies \mathcal{F}[\pi] \models \varphi_{safe}, \varphi_{reach}.$$

4.1.3 DSTS policy synthesis.

In the following, we deem a policy as a function $\pi(\theta)$ of its parameters θ (e.g. the weights of a neural network). We abbreviate $\pi(\theta)$ as π_θ for simplicity. Given a DSTS $\mathcal{F}[\pi_\theta]$, the abstract safety loss function $\mathcal{L}_{\mathcal{D}}$ of $\mathcal{F}[\pi_\theta]$ is essentially a function of the policy π_θ, or more specifically, a function of π_θ's parameters θ. To reduce the abstract safety loss of π_θ, we can leverage a gradient-descent style optimization to update θ by taking steps proportional to the negative of the gradient of $\mathcal{L}_{\mathcal{D}}$ at θ. As opposed to standard gradient descent, we optimize π_θ based on the symbolic rollouts produced by the policy in an abstract domain for $\mathcal{F}[\pi_\theta]$, favouring the abstract interpreter directly for verification-based safe policy synthesis.

We propose a white-box approach for calculating the gradient of the safety loss function $\mathcal{L}_{\mathcal{D}}$ and a black-box approach for estimating the gradient if $\mathcal{L}_{\mathcal{D}}$ is not differentiable.

White-box policy gradient. Our verifier is parametric over an abstract interpreter $\mathcal{D}$, if abstract transformers associated with $\mathcal{D}$ for the policy π_θ and for the state transition function are differentiable, we compute the gradients [48] of the abstract safety loss function $\mathcal{L}_{\mathcal{D}}(\mathcal{F}[\pi_\theta], \varphi_{safe}, \varphi_{reach})$ using off-the-shelf automatic differentiation libraries such as PyTorch [32].

$$\nabla_\theta \mathcal{L}_{\mathcal{D}} \leftarrow \frac{\partial \mathcal{L}_{\mathcal{D}}(\mathcal{F}[\pi_\theta], \varphi_{safe}, \varphi_{reach})}{\partial \theta}$$

Black-box policy gradient. Even in cases when abstract transformers are not differentiable or third-party implementations do not allow differentiation, we can effectively estimate gradients based on random search [29]. Given a DSTS $\mathcal{F}[\pi_\theta]$, at each training iteration, we obtain perturbed DSTSs $\mathcal{F}[\pi_{\theta+\nu\delta}]$ and $\mathcal{F}[\pi_{\theta-\nu\delta}]$ where we add sampled Gaussian noise δ to the current policy π_θ's parameters θ in both directions and ν is a small positive real number. By evaluating the abstract safety losses of the symbolic rollouts of $\mathcal{F}[\pi_{\theta+\nu\delta}]$ and $\mathcal{F}[\pi_{\theta-\nu\delta}]$, we update the policy parameters θ with a finite difference approximation along an unbiased estimator of the policy gradient:

$$\nabla_\theta \mathcal{L}_{\mathcal{D}} \leftarrow \frac{\mathcal{L}_{\mathcal{D}}(\mathcal{F}[\pi_{\theta+\nu\delta}], \varphi_{safe}, \varphi_{reach}) - \mathcal{L}_{\mathcal{D}}(\mathcal{F}[\pi_{\theta-\nu\delta}], \varphi_{safe}, \varphi_{reach})}{\nu}$$

With a policy gradient $\nabla_\theta \mathcal{L}_{\mathcal{D}}$, we update policy parameters θ as below where η is a learning rate:

$$\theta \leftarrow \theta - \eta \cdot \nabla_\theta \mathcal{L}_{\mathcal{D}}$$

4.2 Safe policy synthesis for Unknown Models

As explained in Sec. 2, for unknown or complex nonlinear environments, our approach extends the solution for the deterministic case in Sec. 4.1. The core idea is to learn a time-vary linear Gaussian (TVLG) to approximate unknown environments, based on model-based learning.

In this section, we limit policy synthesis to linear Guassian $\pi(\cdot|s_t) \sim \mathcal{N}(K \cdot s_t + k, S)$ where K and k are parameters and S is a diagonal covariance matrix. Our approach can be easily extended to support time-vary linear-Gaussian policies for increased expressivity. Since both environment models and policies are linear-Gaussian, an MDP system combined of such a model and a policy is still linear-Gaussian.

A state of a TVLG system at timestep t is essentially sampled from a Gaussian distribution. In the following, we directly interpret a concrete TVLG state at timestep t as a Gaussian distribution (μ_{s_t}, Ω_t) where μ_{s_t} denotes the mean of all possible state samples at t and Ω_t denotes the covariance of all such samples.

Definition 4.10 (**TVLG** – Time-varying Linear-Gaussian)**.** Given an MDP $M = (X, S, A, F, S_0, \varphi_{safe}, \varphi_{reach}, R, \beta)$ where the state transition function F is unknown, we approximate M as a TVLG $\mathcal{G}[\cdot] = ((A_t, B_t, c_t, \Sigma_t),\ \cdot,\ (S_0, \Omega_0))$, parameterized by an unknown stochastic policy $\pi(\cdot|s_t) \sim \mathcal{N}(K \cdot s_t + k, S)$, where A_t, B_t, c_t, Σ_t are the time-varying state transition matrices and (S_0, Ω_0) defines the initial states (see below). We explicitly model policy deployment as $\mathcal{G}[\pi] = ((A_t, B_t, c_t, \Sigma_t),\ \pi,\ (S_0, \Omega_0))$. A concrete state at timestep t in a rollout of $\mathcal{G}[\pi]$ is (μ_t, Ω_t), which expresses a multivariate normal distribution $\mathcal{N}(\mu_t, \Omega_t)$, and (μ_{s_0}, Ω_0) is the concrete initial state:

$$\begin{aligned} \mu_{s_0} &= s_0 \wedge s_0 \in S_0 \\ \mu_{a_t} &= K \cdot \mu_{s_t} + k, && \forall t \geq 0 \\ \mu_{s_{t+1}} &= A_t \cdot \mu_{s_t} + B_t \cdot (\mu_{a_t}) + c_t, && \forall t \geq 0 \end{aligned} \tag{3}$$

and

$$\begin{aligned} \Omega_0 &= \left[0\right]_{|S|\times|S|} \\ \Delta_t &= \begin{bmatrix} \Omega_t & \Omega_t \cdot K^T \\ K \cdot \Omega_t & K \cdot \Omega_t \cdot K^T + S \end{bmatrix}, && \forall t \geq 0 \\ \Omega_{t+1} &= \Sigma_t + \left[A_t, B_t\right] \cdot \Delta_t \cdot \left[A_t, B_t\right]^T, && \forall t \geq 0 \end{aligned} \tag{4}$$

4.2.1 Environment Model Inference.

The shape of a TVLG model implies that one can simply use linear regression to fit the model with N rollouts sampled from the actual environment to determine A_t, B_t, c_t, and then fit Σ_t based on the errors. If we take N to be sufficiently large, then any new rollout lies within the confidence interval of the linear-Gaussian model at each timestep t with high probability. However, in practice, we are more interested in learning an accurate model with only a small number of rollouts so that model-based verification is inexpensive. One observation is that environment dynamics at nearby timesteps are often strongly correlated. This means that sample complexity for the local model at a timestep can be reduced if we incorporate information from other timesteps or even models learned from previous training iterations.

We learn the transition matrices by linear regression with a learned Gaussian mixture model (GMM) prior. Following [25], we fit a GMM prior to all of the samples (s_t, a_t, s_{t+1}) at all timesteps from all N trajectories. We then estimate the TVLG dynamics by fitting the linear-Gaussian dynamics for a particular timestep t to the samples at t, conditioned on the GMM prior. This approach makes it feasible to learn TVLG dynamics even with the number of rollouts much lower than the system dimensionality [25].

4.2.2 TVLG Policy Verification.

Given a TVLG dynmaics system $\mathcal{G}[\pi] = ((A_t, B_t, c_t, \Sigma_t), \pi, (S_0, \Omega_0))$, we verify the safety of π using abstract interpretation. Each TVLG state (μ_{s_t}, Ω_t) is interpreted as the mean and covariance of all possible sampled states at timestep t. As defined in Equation (4), since the covariances do not depend on states, we can leave Ω_t *unabstraced* and only choose a suitable abstract domain for the means μ_{s_t}, which are state-dependent. The transition matrices (A_t, B_t, c_t) define a deterministic state transition system for μ_{s_t} in Equation (3), which means that we can reduce TVLG verification to DSTS abstract interpretation.

TVLG Symbolic Rollout. Given a TVLG system $\mathcal{G}[\pi]$, let $\mathcal{D} = \langle \mathcal{D}_c \equiv S, \mathcal{D}_a, \alpha, \gamma, f \equiv \{(+, \oplus), (\cdot, \odot)\}\rangle$ be an instantiated abstract interpreter for the state transition system in Equation (3) for μ_{s_t}, the means of all possible sampled states at a timestep t. Here $\oplus$ and $\odot$ are suitable abstract transformers for matrix sum + and multiplication $\cdot$ in the chosen abstract domain $\mathcal{D}_a$. $\mathcal{G}[\pi]$'s symbolic rollout is a sequence of abstract states $S_0^{\mathcal{D}} = (\mu_{S_0}^{\mathcal{D}}, \Omega_0), S_1^{\mathcal{D}} = (\mu_{S_1}^{\mathcal{D}}, \Omega_1), \ldots, S_T^{\mathcal{D}} = (\mu_{S_T}^{\mathcal{D}}, \Omega_T)$, where $\Omega_0, \Omega_1, \ldots, \Omega_T$ are covariances from equations (4) and $\mu_{S_t}^{\mathcal{D}}$ is the abstraction of μ_{s_t}:

$$
\begin{aligned}
\mu_{S_0}^{\mathcal{D}} &= \alpha(S_0) \\
\mu_{A_t}^{\mathcal{D}} &= \left(K \odot \mu_{S_t}^{\mathcal{D}}\right) \oplus k, && \forall t \geq 0 \\
\mu_{S_{t+1}}^{\mathcal{D}} &= \left(A_t \odot \mu_{S_t}^{\mathcal{D}}\right) \oplus \left(B_t \odot \left(\mu_{A_t}^{\mathcal{D}}\right)\right) \oplus c_t, && \forall t \geq 0 \qquad (5)
\end{aligned}
$$

For exposition purpose, we lift the abstraction function α for μ_{s_t} to an abstraction function $\hat{\alpha}$ for a TVLG state. Given a TVLG state (μ_{s_t}, Ω_t) at a timestep t, $\hat{\alpha}(\mu_{s_t}, \Omega_t) = (\alpha(\{\mu_{s_t}\}), \Omega_t)$. Similarly, we define the concretization function for an abstract TVLG state $S_t^{\mathcal{D}} = (\mu_{S_t}^{\mathcal{D}}, \Omega_t)$ simply as $\hat{\gamma}(S_t^{\mathcal{D}}) = (\gamma(\mu_{S_t}^{\mathcal{D}}), \Omega_t)$.

4.2.3 TVLG Policy Safety Loss.

Similar to DSTS verification (Definition 4.8), to compute the worst-case safety loss among all sampled states subsumed by an abstract TVLG state $S_t^{\mathcal{D}} = (\mu_{S_t}^{\mathcal{D}}, \Omega_t)$ with respect to a safety property, we approximate $\hat{\gamma}(S_t^{\mathcal{D}})$ with a tight interval concretization $\hat{\gamma}_I(S_t^{\mathcal{D}})$. Because the value of each sampled state at timestep t is affected by the covariance Ω_t as well, we must take sampled states that deviate from the means into account.

Recall that a TVLG state s can be considered sampled from a joint Gaussian distribution $\mathcal{N}(\mu_s, \Omega)$ with mean μ_s. The main diagonal (*diag*) of the covariance matrix Ω contains the variance of each state dimension. Ideally one could use a confidence hyper-ellipse (whose shape is determined by the eigenvectors and eigenvalues of Ω) to define the region that contains all states that can be drawn from the joint Gaussian distribution with high probability. For efficient verification, we instead use an interval (box) estimation to bound the confidence hyper-ellipse for approximating deviated states. A normal deviated state s lies within the interval range between $\left[\mu_s - n \cdot \sqrt{diag(\Omega)}, \mu_s + n \cdot \sqrt{diag(\Omega)}\right]$ with high probability. Here n is a parameter used to parameterize the probabilistic coverage of deviated samples from the mean μ_s. For example, taking $n = 5$ accounts for 99.99% of all the possible deviated states.

Given an abstract state $S^D = (\mu_S^{\mathcal{D}}, \Omega)$ of a TVLG system, define $\hat{\gamma}_I^n(S^D)$ as its approximated interval concretization:

$$
\hat{\gamma}_I^n(S^{\mathcal{D}}) = \hat{\gamma}_I^n((\mu_S^{\mathcal{D}}, \Omega)) = (l - n \cdot \sqrt{diag(\Omega)}, u + n \cdot \sqrt{diag(\Omega)})
$$

where $(l, u) = \gamma_I(\mu_S^{\mathcal{D}})$. Intuitively, since $\gamma_I(\mu_S^{\mathcal{D}})$ is the interval lower and upper bound of all concrete means over-approximated by the mean abstraction $\mu_S^{\mathcal{D}}$, further subtracting to the lower bound and adding to the upper bound a standard deviation yields an interval estimation of a probabilistic coverage of all sampled states that deviate from the concrete means constrained by Ω.

Given a safety property φ, the abstract safety loss function $\mathcal{L}_{\mathcal{D}}(S^{\mathcal{D}}, \varphi)$ for a TVLG abstract state $S^{\mathcal{D}}$ is defined as:

$$
\mathcal{L}_{\mathcal{D}}(S^{\mathcal{D}}, \varphi) = \max_{s \in \hat{\gamma}_I^n(S^{\mathcal{D}})} (\mathcal{L}(s, \varphi))
$$

The computation of this function is the same as Definition 4.6. We formally characterize its soundness property below:

Theorem 4.11 (Abstract Safety Loss Function Soundness)**.** *Given an abstract TVLG state* $(\mu_S^{\mathcal{D}}, \Omega)$ *and a safety property* φ*, we have*

$$
\mathcal{L}_{\mathcal{D}}((\mu_S^{\mathcal{D}}, \Omega), \varphi) = 0 \implies s \models \varphi \; \forall s \in \hat{\gamma}_I^n(\mu_S^{\mathcal{D}}, \Omega).
$$

Our TVLG verification is essentially probabilistic and we use the parameter n to adjust the probabilistic coverage of

deviated states from the Gaussian means. Under a chosen probabilistic coverage, given a time horizon T, a TVLG $\mathcal{G}[\pi]$ satisfies safety properties φ_{safe} and φ_{reach}, iff for its symbolic rollout $S_0^{\mathcal{D}}, S_1^{\mathcal{D}}, \ldots, S_{T-1}^{\mathcal{D}}, S_T^{\mathcal{D}}$ there exists $T' \leq T$ such that:

$$\underbrace{S_0^{\mathcal{D}}, S_1^{\mathcal{D}}, \ldots, S_{T'-1}^{\mathcal{D}}}_{\forall t \in 1 \ldots T'-1,\ \mathcal{L}_{\mathcal{D}}(S_t^{\mathcal{D}}, \varphi_{safe})=0} \quad \underbrace{S_{T'}^{\mathcal{D}}}_{\mathcal{L}_{\mathcal{D}}(S_{T'}^{\mathcal{D}}, \varphi_{reach})=0}$$

If the symbolic rollout is unsafe, the abstract safety loss of $\mathcal{G}[\pi]$ is:

$$\mathcal{L}_{\mathcal{D}}(\mathcal{G}[\pi], \varphi_{safe}, \varphi_{reach}) = \mathcal{L}_{\mathcal{D}}(S_T^{\mathcal{D}}, \varphi_{reach}) + \textstyle\sum_{t=1}^{T} \mathcal{L}_{\mathcal{D}}(S_t^{\mathcal{D}}, \varphi_{safe})$$

4.2.4 TVLG Safe policy synthesis.

A policy $\pi_\theta(\cdot|s_t) \sim \mathcal{N}(K \cdot s_t + k, S)$ is deemed as a function of its parameters θ. Policy parameters θ include K, k and S. We could simply run gradient descent on the loss function $\mathcal{L}_{\mathcal{D}}(\mathcal{G}[\pi_\theta], \varphi_{safe}, \varphi_{reach})$ to update θ to reduce safety loss, however, a policy update as such can change the behavior of π_θ arbitrarily different from the old one at each training iteration. Because the fitted TVLG dynamics $\mathcal{G}[\cdot]$ is a local model and only valid in a local region of the state space around the sampled rollouts, an unconstrained parameter update can cause the new policy to visit part of the state space where $\mathcal{G}[\cdot]$ is arbitrarily incorrect and unstable, leading to divergence. Therefore, our approach restricts the change of policies at each iteration to maintain the validity of a fitted time-varying linear model $\mathcal{G}[\cdot]$. Inspired by a few recently developed RL algorithms [22, 35], we address this issue by limiting the change by imposing a constraint on the KL-divergence between the old policy $\pi_{\theta_{old}}$ and the new policy π_θ by a threshold δ:

$$\begin{aligned} &\min_\theta \mathcal{L}_{\mathcal{D}}(\mathcal{G}[\pi_\theta], \varphi_{safe}, \varphi_{reach}) \\ &\textit{subject to}\, \mathbb{E}_{s \sim d^{\pi_{\theta_{old}}}}[D_{KL}(\pi_{\theta_{old}}(\cdot|s) \,||\, \pi_\theta(\cdot|s))] \leq \delta \end{aligned} \tag{6}$$

where $d^{\pi_{\theta_{old}}}$ is the state distribution under the policy $\pi_{\theta_{old}}$ in the actual (true) environment[3] and the KL divergence D_{KL} is the expectation of the logarithmic difference between the probabilities of $\pi_{\theta_{old}}$ and π_θ:

$$D_{KL}(\pi_{\theta_{old}} \,||\, \pi_\theta) = \mathbb{E}_{x \sim \pi_{\theta_{old}}}\left(\log \frac{\pi_{\theta_{old}}(x)}{\pi_\theta(x)}\right)$$

here the expectation is taken using the probabilities of $\pi_{\theta_{old}}$. Intuitively, D_{KL} measures how the probability distribution $\pi_{\theta_{old}}$ is different from a new policy π_θ.

The constrained optimization problem (6) can be analytically solved (similar to [22, 35]). We update θ as below. The derivation of this solution is given in Appendix A.3.

$$\begin{aligned} &\theta = \theta_{old} - \sqrt{\frac{2\delta}{g^T H(\theta_{old})^{-1} g}} H(\theta_{old})^{-1} g \\ &\textit{where}\ g = \nabla_\theta \mathcal{L}_{\mathcal{D}}(\mathcal{G}[\pi_\theta], \varphi_{safe}, \varphi_{reach})|_{\theta=\theta_{old}} \end{aligned} \tag{7}$$

[3] $d^\pi(s) = P(s_0 = s) + \beta P(s_1 = s) + \beta^2 P(s_2 = s) + \cdots$ where $s_0 \in S_0$, and $a_t \sim \pi(\cdot|s_t)$, $s_{t+1} \sim P(s_{t+1}|s_t, a_t)\ \forall t \geq 0$. If $\beta = 1$, $d_{\pi_{\theta_{old}}}$ is just the state visit frequency under $\pi_{\theta_{old}}$. P is the true transition probability distribution.

Require: MDP M as $(X, S, A, F, S_0, \varphi_{safe}, \varphi_{reach}, R)$ where the environment dynamics (state transition) function F is unknown, initial policy π_θ, KL divergence threshold δ.
Ensure: Optimized policy π_θ and a learned TVLG model $\mathcal{G}[\cdot]$ such that $\mathcal{G}[\pi_\theta] \models \varphi_{safe}, \varphi_{reach}$.

procedure MARVEL
  $\theta \leftarrow$ all weights in π_θ to optimize
  while `true` **do**
    Collect set of trajectories $\mathcal{S}$ on policy π_θ
    Fit the TVLG dynamics $\mathcal{G}[\cdot]$ to the samples $\mathcal{S}$
      ▷ Abstract Interpretation
    $\ell_{\mathcal{D}} \leftarrow \mathcal{L}_{\mathcal{D}}(\mathcal{G}[\pi_\theta], \varphi_{safe}, \varphi_{reach})$
    if $\ell_{\mathcal{D}} = 0$ **then**
      Dump π_θ and $\mathcal{G}[\cdot]$ to a safe policy list
    end if
      ▷ Abstraction for Training
    $\theta_{old} \leftarrow \theta$
    Estimate $H(\theta_{old})$ based on the samples $\mathcal{S}$
    $g \leftarrow \nabla_\theta \mathcal{L}_{\mathcal{D}}(\mathcal{G}[\pi_\theta], \varphi_{safe}, \varphi_{reach})|_{\theta=\theta_{old}}$
    $\theta \leftarrow \theta_{old} - \sqrt{\frac{2\delta}{g^T H(\theta_{old})^{-1} g}} H(\theta_{old})^{-1} g$
    Off-policy RL update on θ with $\mathcal{S}$ and reward R
  end while
end procedure

Figure 3. Marvel: Verification-guided safe policy training.

$H(\theta_{old})$ is a Hessian matrix that measures the second-order derivative of the log probability of $\pi_{\theta_{old}}$ (after extending the KL divergence definition). Importantly, as opposed to improving policy parameters simply using the abstract safety loss gradient $\nabla_\theta \mathcal{L}_{\mathcal{D}}$, the update rule in Equation (7) uses an additional KL divergence threshold δ to restrain policy updates that can turn destructive to the validity of the fitted TVLG model $\mathcal{G}[\cdot]$. For sample efficiency, since $H(\theta_{old})$ is estimated based on sampled states from the old policy $\pi_{\theta_{old}}$, we can reuse the samples used to fit the TVLG model $\mathcal{G}[\cdot]$ for estimating $H(\theta_{old})$.

4.2.5 Model-free Modal-based Safe policy synthesis.

We have presented a verification-based policy update approach that improves the safety of a policy even in environments with unknown dynamics. It requires that every update be consistent with a learned TVLG model. Initially the model could be far away from a good assumption and hence it would require a large number of training iterations to converge. Moreover, it does not incorporate MDP reward functions R which may include performance constraints other than safety constraints. To accelerate learning and integrate MDP reward signals R, we alternate our model-based policy update with model-free reinforcement learning, combining the strong safety guarantee of our model-based approach with the performance advantages of model-free RL.

Since both the model-free and model-based approaches need rollouts data to estimate policy gradients, one challenge of designing an integrated approach is sample efficiency. To address this, after a model-based policy update, we do not sample new rollouts from the updated policy π_θ for model-free learning. Instead, we reuse the samples from the old policy $\pi_{\theta_{old}}$ (used to fit the TVLG $\mathcal{G}[\cdot]$) for an *off-policy* model-free RL update with importance sampling. The goal is to update θ to maximize the long term reward ([22, 35]) $\mathbb{E}_{s\sim d^{\pi_{\theta_{old}}}, a\sim\pi_{\theta_{old}}(\cdot|s)}\left[\frac{\pi_\theta(a|s)}{\pi_{\theta_{old}}(a|s)} A^{\pi_{\theta_{old}}}(s,a)\right]$ where advantage rewards $A^{\pi_{\theta_{old}}}$ ([23]) can be estimated based on the $\pi_{\theta_{old}}$ samples using an advantage estimation algorithm [22, 35]. Importance sampling works well at this step as we have penalized large KL divergence between $\pi_{\theta_{old}}$ and π_θ in Equation (6).

Marvel's model-free model-based safe policy synthesis algorithm is given in Figure 3. The goal is to optimize the policy π_θ and also learn a TVLG model $\mathcal{G}[\cdot]$ for an MDP M. Policy search aims to have $\mathcal{L}_\mathcal{D}(\mathcal{G}(\pi_\theta), \varphi_{safe}, \varphi_{reach})$ reduced to 0, thereby ensuring π_θ safe with respect to the TVLG model $\mathcal{G}[\cdot]$ fitted at line 5 and the safety properties. The policy's abstract safety loss, denoted as $\ell_\mathcal{D}$, is computed at Line 6. If $\ell_\mathcal{D} = 0$, Marvel dumps the safe policy as well as the learned TVLG model. The abstract safety loss $\ell_\mathcal{D}$ is used to guide the search of policy parameters at Line 12 to Line 13 according to Equation (7). Finally, at Line 14, we update the policy π_θ with the samples from $\pi_{\theta_{old}}$ using off-policy model-free RL for sample efficiency.

5 Experimental Results

We have implemented our verification-based safe policy synthesis algorithm (Fig. 3) in a tool called Marvel. For abstract interpretation, Marvel uses the Zonotope abstract domain to reason about nonlinear state transition dynamics [4] and the DeepPoly abstract domain [37] to reason about control polices (including neural network policies). Marvel uses natural policy gradient (NPG) [22, 35] to support the off-policy RL update in line 14 of our algorithm in Fig. 3.

Baseline. Our baseline is a variant of Marvel that disables model-based learning and the verification-based update from line 5 to line 13 of the algorithm in Fig. 3. Under this condition, Marvel is equivalent to the NPG learning algorithm. We aim to demonstrate that the safety guarantee provided by Marvel can lead to safe policies in scenarios that fail the baseline. We shaped the reward functions for Marvel and the baseline so that they have a penalty for states that do not satisfy φ_{safe} or φ_{reach}. We do not include a comparison with the previous TVLG-based RL algorithm [25] because Marvel significantly outperforms it on our benchmarks.

5.1 Deterministic State Transition Systems

Neural Network Policies. In our first experiment, we evaluated Marvel on a diverse set of real-world cyber-physical system benchmarks with known state-transition dynamics, taken from the literature [1]. For all the benchmarks, φ_{safe} is a conjunction of interval constraints over system variables, meaning that the goal is to learn a policy that can maintain the system within a safety boundary. Similar to the CartPole problem in Sec.2, to prove that φ_{safe} holds in infinite timesteps, we set φ_{reach} as an inductive invariant, logically equivalent to the set of initial states, requiring that any rollout starting from a state in φ_{reach} eventually turns back to φ_{reach} and does not encounter a state that fails φ_{safe}. The polices are all two-layer neural networks (4×4) with tanh activation functions. Marvel was run without TVLG inference because the environment models are known.

Table 1. Safe policy synthesis with neural networks. Dim is the number of variables. AbsLoss is the best abstract safety loss achieved in training. K is the number of steps a verified policy can steer back to an inductive invariant. Iters is the number of iterations to find a verifiably safe policy.

Benchmark	Dim	Baseline AbsLoss	Marvel K	Marvel Iters
MagneticSup	2	33.78	1	352
Pendulum	2	2.03	3	400
Satellite	2	6.17	3	224
Helicopter	3	0.43	3	574
MagneticPtr	3	0.47	9	859
InverPendulum	4	0.31	3	1738
4CarPlatoon	8	1.33	10	121

The result is listed in Table 1. Marvel was able to produce verifiably safe neural policies for all the considered benchmarks. Although on most benchmarks the NPG baseline can achieve similar rewards to Marvel, the learned policies cannot be verified safe. This is because the baseline policies were not trained with verification feedback and can converge to arbitrary policy parameters; abstract interpretation produced very conservative abstractions for their tanh functions that failed verification. Marvel can use verification feedback to learn well-performing policies that additionally allow tight abstractions for the neural network policies.

Nonlinear Continuous Systems. We also evaluated Marvel on two *nonlinear* continuous cyber-physical systems taken from the ARCH-COMP'20 competition [21]. Adaptive Cruise Control System (ACC) involves an ego vehicle and a lead vehicle with six variables representing the position, velocity and acceleration of the two vehicles. Our training objective is to learn a linear policy that, when the lead vehicle suddenly reduces its speed, the ego car can decelerate to maintain a safe distance. φ_{safe} specifies the minimum relative distance that a policy should maintain at each timestep as well as an upper bound to prevent the ego car from stopping. A rollout lasts 50 timesteps and each timestep is 0.1s. Figure. 4 depicts the training performance of Marvel where we show the abstract safety loss at each training iteration. The baseline

(blue) failed to further significantly reduce the worst-case safety loss. Marvel (olive) learned a safe policy at 63 iteration because it uses verification feedback to directly optimize the worst-case safety loss. Previous work [41] used verification to detect safety issues for a well-trained policy for the ACC system. Our result shows that verification can also be used for policy safe-by-construction. The result for the second nonlinear benchmark Single Pendulum is left in Appendix A.2.

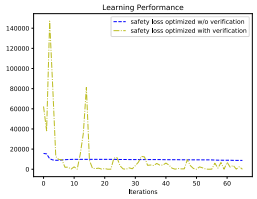

Figure 4. ACC Training.

5.2 MDPs with unknown or complex dynamics

We evaluated Marvel under the condition that either an MDP's state transition function is unknown or its complex dynamics does not allow scalable verification. We collected a large set of RL benchmarks including classic control problems and robotics applications. We highlight a few representative benchmarks. The full description is in Appendix A.4.

The result is depicted in Fig. 5 where we compare the policies learned using Marvel against that learned using the baseline in terms of their abstract safety loss during training. We also depict the result of running abstract interpretation over a learned environment model and a learned policy as a combined closed-loop system for two benchmarks in Fig. 6. We draw the interval concretization of each abstract state as well as concrete rollouts from the real environments. The results suggest that Marvel achieved zero abstract safety loss and learned accurate environment models. For most of these benchmarks, the baseline failed to learn a verifiably safe policy even if we doubled the training episodes.

The first benchmark ACC taken from [6] models a variant of the adaptive cruise control system. The lead car can apply an acceleration at any time. The goal is to follow a lead car as closely as possible. Fig. 6a shows that the relative vehicle positions in all sampled rollouts are safe and subsumed by the abstraction. Without model-based learning and verification, the baseline cannot guarantee safety as depicted in Fig. 5a. We found that the baseline policies can accelerate quickly to catch up the lead car to achieve a high reward but fail to slow down soon enough to avoid a crash. This result demonstrates that integrating safety verification into the policy training loop can correct policy search directions toward safe policies.

We observed similar results for Obstacle taken from [6], Airplane from the ARCH-COMP'20 competition [21], and DoublePendulum and Hopper from Mujoco [40]. For Obstacle, Marvel learned safe policies that can arrive a goal state without hitting obstacles, a behavior that the baseline failed to reinforce as depicted in Fig. 5b. The safety property of Airplane is that the Euler angles during flight must be between $[-1, 1]^3$. DoublePendulum is a harder version of the CartPole problem, where the pole has another pole on top of it. Verification feedback again is the key for safe policy synthesis as shown in Fig. 5c and Fig. 5d.

The training objective of Hopper is to make a one-legged robot hop as fast as possible. Its safety property is that the robot height is always greater than 0.7 and the robot angle is smaller than 0.2. A rollout lasts 500 timesteps. NPG exploration failed to learn a safe policy and encountered large safety penalty during training. Marvel was much more stable in training. We therefore show the average rewards (including safety rewards) collected by both algorithms instead and leave the abstract safety loss comparison in Appendix. A.4. Fig. 5e indicates that Marvel outperforms the baseline significantly. We depict the abstraction of robot heights in Fig. 6b.

Thrower is a 19-dimensional benchmark taken from Mujoco [40]. The goal is to manipulate a robotic arm to hit a ball to goal areas, specified as φ_{reach}. The learning curve of Marvel for this benchmark is more stable than the baseline as shown in Fig. 5f. We show the results of the other two Mujoco benchmarks, Reacher and Pusher, in Appendix. A.4.

Model accuracy. An environment model is *accurate* if sampled rollouts lie within the interval conretization of a system's symbolic rollouts. Marvel only samples 50 rollouts to learn an environment model at each training iteration. This is to ensure that model-based verification is inexpensive. It learned fully accurate models for low-dimensional benchmarks such as ACC, Obstacle and DoublePendulum (measured by sampling). We quantify the model accuracy for some high-dimensional benchmarks below. For each system, we sampled 1000 rollouts to count the states for which the learned model is inaccurate. These states fall out of the interval concretization of the system's abstraction.

The model of Hopper (11 dimensions) is inaccurate only at **0.37%** of the sampled states. The Thrower model (19 dimensions) has a **0.007%** low inaccuracy rate, the Pusher model (20 dimensions) has **1.17%** inaccuracy rate, and the Reacher model (9 dimensions) has **0%** inaccuracy rate. A sampled rollout rarely leaves the interval concretizations of system abstraction. Even if a sampled rollout temporarily falls out of the interval concretization at a timestep, the leave is marginal and the rollout eventually comes back.

6 Related Work

Robust Machine Learning. Our work on using abstract interpretation [12] for safe policy synthesis is inspired by the recent advances in verifying neural network robustness, e.g. [5, 18, 37, 47]. These approaches apply abstract transformers to relax nonlinearity of activation functions in a neural network into convex representations, based on linear approximation [36, 37, 47, 49, 51] or interval approximation [19, 30]. Since the abstractions are differentiable, neural networks can be optimized toward tighter concertized bounds to improve verified robustness [7, 28, 30, 45, 51]. These approaches do

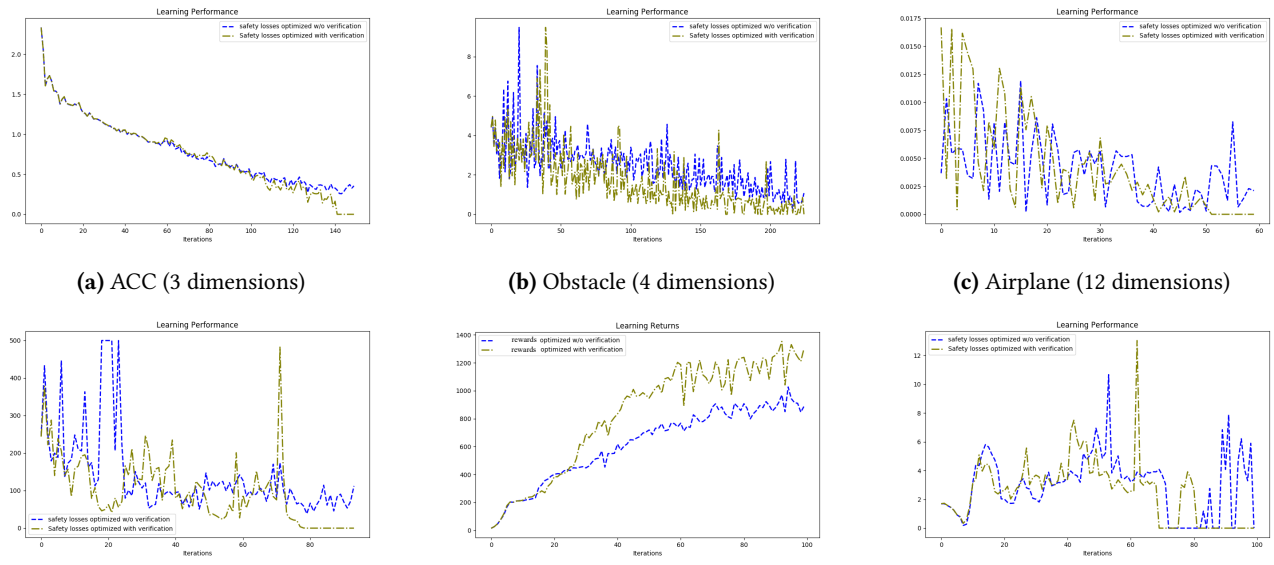

(a) ACC (3 dimensions) **(b)** Obstacle (4 dimensions) **(c)** Airplane (12 dimensions)

(d) DoublePendulum (6 dimensions) **(e)** Hopper (11 dimensions) **(f)** Thrower (19 dimensions)

Figure 5. Comparison between Marvel (olive) and the baseline (blue) in terms of policy abstract safety losses / rewards.

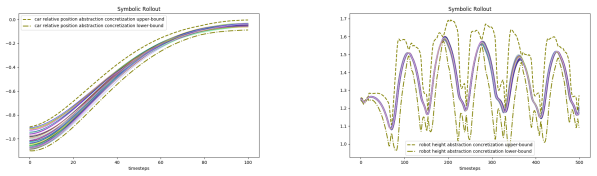

(a) ACC **(b)** Hopper

Figure 6. Abstract interpretation: interval concretization of abstract states (olive dashed lines) and sampled rollouts (colored trajectories) from the real environments are depicted.

not consider the environment in which a neural network is deployed. Safety verification of a control policy over a time horizon with complex system dynamics remains challenging.

Recent work [14, 15, 20, 39, 41] achieved initial results about verifying learning-enabled autonomous systems. However, these approaches do not attempt to perform verification within a learning loop. Marvel demonstrates the substantial benefits of training policies with verification feedback.

Safe Reinforcement Learning. Safe reinforcement learning is a fundamental problem in machine learning [31, 42]. Verification is considered in [3] but the focus is on stability. Most safe RL algorithms form a constraint optimization problem specifying safety constraints as a cost function in addition to an objective reward function [2, 9, 13, 24, 26]. Their goal is to train a policy that maximizes the accumulated reward and bounds the amount of safety violation under a threshold. In contrast, Marvel ensures that a learned policy is formally verified safe with respect to an environment model. Model-based safe learning was previously combined with formal verification in [17]. However, a hand-crafted global model is required, which is updated as learning progresses to take into account the deviations between the model and the actual system behavior. Marvel infers environment models locally from data. Our contribution is significant because, without a global model, even small policy updates can cause safety guarantees based on a local model incorrect.

Revel [6] introduces a mechanism to learn neural-symbolic RL agents to ensure safe exploration during training. Similar approaches [8, 44, 52] synthesize a symbolic program to approximate an RL policy based on imitation learning [34] and show that the symbolic program can be used to replace the RL policy for better interpretability and safety. In contrast, Marvel focuses on direct learning of verifiably safe policies by integrating verification into a policy learning loop.

7 Conclusions

We present Marvel that bridges policy synthesis and verification for control policy safe-by-construction. Formal verification is integrated into a policy learning loop using symbolic counterexample-guided inductive synthesis. Our experiments demonstrate that policy updates based on verification feedback can lead to provably safe policies.

For future work, we plan to extend Marvel to support policy safety during exploration. When a worst-case environment model is provided, this can be achieved by firstly performing a policy update to maximize the long-term reward and then reconciling the safety violation by projecting the policy back onto the verified safe space [11].

References

[1] Alessandro Abate, Iury Bessa, Dario Cattaruzza, Lucas Cordeiro, Cristina David, Pascal Kesseli, Daniel Kroening, and Elizabeth Polgreen. 2017. Automated Formal Synthesis of Digital Controllers for State-Space Physical Plants. In *Computer Aided Verification (CAV) (LNCS, Vol. 10426)*. Springer, 462–482.

[2] Joshua Achiam, David Held, Aviv Tamar, and Pieter Abbeel. 2017. Constrained Policy Optimization. In *Proceedings of the 34th International Conference on Machine Learning, ICML 2017, Sydney, NSW, Australia, 6-11 August 2017 (Proceedings of Machine Learning Research, Vol. 70)*, Doina Precup and Yee Whye Teh (Eds.). PMLR, 22–31. http://proceedings.mlr.press/v70/achiam17a.html

[3] Anayo K. Akametalu, Shahab Kaynama, Jaime F. Fisac, Melanie Nicole Zeilinger, Jeremy H. Gillula, and Claire J. Tomlin. 2014. Reachability-based safe learning with Gaussian processes. In *53rd IEEE Conference on Decision and Control, CDC 2014, Los Angeles, CA, USA, December 15-17, 2014*. IEEE, 1424–1431. https://doi.org/10.1109/CDC.2014.7039601

[4] M. Althoff. 2015. An Introduction to CORA 2015. In *Proc. of the Workshop on Applied Verification for Continuous and Hybrid Systems*.

[5] Greg Anderson, Shankara Pailoor, Isil Dillig, and Swarat Chaudhuri. 2019. Optimization and abstraction: a synergistic approach for analyzing neural network robustness. In *Proceedings of the 40th ACM SIGPLAN Conference on Programming Language Design and Implementation, PLDI 2019, Phoenix, AZ, USA, June 22-26, 2019*. 731–744. https://doi.org/10.1145/3314221.3314614

[6] Greg Anderson, Abhinav Verma, Isil Dillig, and Swarat Chaudhuri. 2020. Neurosymbolic Reinforcement Learning with Formally Verified Exploration. *CoRR* abs/2009.12612 (2020). arXiv:2009.12612 https://arxiv.org/abs/2009.12612

[7] Mislav Balunovic and Martin T. Vechev. 2020. Adversarial Training and Provable Defenses: Bridging the Gap. In *8th International Conference on Learning Representations, ICLR 2020, Addis Ababa, Ethiopia, April 26-30, 2020*. OpenReview.net. https://openreview.net/forum?id=SJxSDxrKDr

[8] Osbert Bastani, Yewen Pu, and Armando Solar-Lezama. 2018. Verifiable Reinforcement Learning via Policy Extraction. In *Advances in Neural Information Processing Systems 31: Annual Conference on Neural Information Processing Systems 2018, NeurIPS 2018, 3-8 December 2018, Montréal, Canada*, Samy Bengio, Hanna M. Wallach, Hugo Larochelle, Kristen Grauman, Nicolò Cesa-Bianchi, and Roman Garnett (Eds.). 2499–2509. http://papers.nips.cc/paper/7516-verifiable-reinforcement-learning-via-policy-extraction

[9] Felix Berkenkamp, Matteo Turchetta, Angela P. Schoellig, and Andreas Krause. 2017. Safe Model-based Reinforcement Learning with Stability Guarantees. In *Advances in Neural Information Processing Systems 30: Annual Conference on Neural Information Processing Systems 2017, 4-9 December 2017, Long Beach, CA, USA*, Isabelle Guyon, Ulrike von Luxburg, Samy Bengio, Hanna M. Wallach, Rob Fergus, S. V. N. Vishwanathan, and Roman Garnett (Eds.). 908–918. http://papers.nips.cc/paper/6692-safe-model-based-reinforcement-learning-with-stability-guarantees

[10] Greg Brockman, Vicki Cheung, Ludwig Pettersson, Jonas Schneider, John Schulman, Jie Tang, and Wojciech Zaremba. 2016. OpenAI Gym. arXiv:1606.01540 [cs.LG]

[11] Yinlam Chow, Ofir Nachum, Aleksandra Faust, Mohammad Ghavamzadeh, and Edgar A. Duéñez-Guzmán. 2019. Lyapunov-based Safe Policy Optimization for Continuous Control. *CoRR* abs/1901.10031 (2019). arXiv:1901.10031 http://arxiv.org/abs/1901.10031

[12] Patrick Cousot and Radhia Cousot. 1977. Abstract Interpretation: A Unified Lattice Model for Static Analysis of Programs by Construction or Approximation of Fixpoints. In *Conference Record of the Fourth ACM Symposium on Principles of Programming Languages, Los Angeles, California, USA, January 1977*. 238–252. https://doi.org/10.1145/512950.512973

[13] Gal Dalal, Krishnamurthy Dvijotham, Matej Vecerík, Todd Hester, Cosmin Paduraru, and Yuval Tassa. 2018. Safe Exploration in Continuous Action Spaces. *CoRR* abs/1801.08757 (2018). arXiv:1801.08757 http://arxiv.org/abs/1801.08757

[14] Souradeep Dutta, Xin Chen, and Sriram Sankaranarayanan. 2019. Reachability analysis for neural feedback systems using regressive polynomial rule inference. In *Proceedings of the 22nd ACM International Conference on Hybrid Systems: Computation and Control, HSCC 2019, Montreal, QC, Canada, April 16-18, 2019*, Necmiye Ozay and Pavithra Prabhakar (Eds.). ACM, 157–168. https://doi.org/10.1145/3302504.3311807

[15] Jiameng Fan, Chao Huang, Xin Chen, Wenchao Li, and Qi Zhu. 2020. ReachNN*: A Tool for Reachability Analysis of Neural-Network Controlled Systems. In *Automated Technology for Verification and Analysis - 18th International Symposium, ATVA 2020, Hanoi, Vietnam, October 19-23, 2020, Proceedings (Lecture Notes in Computer Science, Vol. 12302)*, Dang Van Hung and Oleg Sokolsky (Eds.). Springer, 537–542. https://doi.org/10.1007/978-3-030-59152-6_30

[16] Vincent François-Lavet, Peter Henderson, Riashat Islam, Marc G. Bellemare, and Joelle Pineau. 2018. An Introduction to Deep Reinforcement Learning. *Foundations and Trends® in Machine Learning* 11, 3-4 (2018), 219–354. https://doi.org/10.1561/2200000071

[17] Nathan Fulton and André Platzer. 2019. Verifiably Safe Off-Model Reinforcement Learning. In *Tools and Algorithms for the Construction and Analysis of Systems - 25th International Conference, TACAS 2019, Held as Part of the European Joint Conferences on Theory and Practice of Software, ETAPS 2019, Prague, Czech Republic, April 6-11, 2019, Proceedings, Part I (Lecture Notes in Computer Science, Vol. 11427)*, Tomás Vojnar and Lijun Zhang (Eds.). Springer, 413–430. https://doi.org/10.1007/978-3-030-17462-0_28

[18] Timon Gehr, Matthew Mirman, Dana Drachsler-Cohen, Petar Tsankov, Swarat Chaudhuri, and Martin T. Vechev. 2018. AI2: Safety and Robustness Certification of Neural Networks with Abstract Interpretation. In *2018 IEEE Symposium on Security and Privacy, SP 2018, Proceedings, 21-23 May 2018, San Francisco, California, USA*. 3–18. https://doi.org/10.1109/SP.2018.00058

[19] Sven Gowal, Krishnamurthy Dvijotham, Robert Stanforth, Rudy Bunel, Chongli Qin, Jonathan Uesato, Relja Arandjelovic, Timothy A. Mann, and Pushmeet Kohli. 2018. On the Effectiveness of Interval Bound Propagation for Training Verifiably Robust Models. *CoRR* abs/1810.12715 (2018). arXiv:1810.12715 http://arxiv.org/abs/1810.12715

[20] Radoslav Ivanov, James Weimer, Rajeev Alur, George J. Pappas, and Insup Lee. 2018. Verisig: verifying safety properties of hybrid systems with neural network controllers. *CoRR* abs/1811.01828 (2018). arXiv:1811.01828 http://arxiv.org/abs/1811.01828

[21] Taylor T Johnson, Diego Manzanas Lopez, Patrick Musau, Hoang-Dung Tran, Elena Botoeva, Francesco Leofante, Amir Maleki, Chelsea Sidrane, Jiameng Fan, and Chao Huang. 2020. ARCH-COMP20 Category Report: Artificial Intelligence and Neural Network Control Systems (AINNCS) for Continuous and Hybrid Systems Plants. In *ARCH20. 7th International Workshop on Applied Verification of Continuous and Hybrid Systems (ARCH20) (EPiC Series in Computing, Vol. 74)*, Goran Frehse and Matthias Althoff (Eds.). EasyChair, 107–139. https://doi.org/10.29007/9xgv

[22] Sham Kakade. 2001. A Natural Policy Gradient. In *Proceedings of the 14th International Conference on Neural Information Processing Systems: Natural and Synthetic* (Vancouver, British Columbia, Canada) *(NIPS'01)*. MIT Press, Cambridge, MA, USA, 1531–1538.

[23] Sham M. Kakade and John Langford. 2002. Approximately Optimal Approximate Reinforcement Learning. In *Machine Learning, Proceedings of the Nineteenth International Conference (ICML 2002), University of New South Wales, Sydney, Australia, July 8-12, 2002*, Claude Sammut and Achim G. Hoffmann (Eds.). Morgan Kaufmann, 267–274.

[24] Hoang Minh Le, Cameron Voloshin, and Yisong Yue. 2019. Batch Policy Learning under Constraints. In *Proceedings of the 36th International*

Conference on Machine Learning, ICML 2019, 9-15 June 2019, Long Beach, California, USA (Proceedings of Machine Learning Research, Vol. 97), Kamalika Chaudhuri and Ruslan Salakhutdinov (Eds.). PMLR, 3703–3712. http://proceedings.mlr.press/v97/le19a.html

[25] Sergey Levine and Pieter Abbeel. 2014. Learning Neural Network Policies with Guided Policy Search under Unknown Dynamics. In *Advances in Neural Information Processing Systems 27: Annual Conference on Neural Information Processing Systems 2014, December 8-13 2014, Montreal, Quebec, Canada*, Zoubin Ghahramani, Max Welling, Corinna Cortes, Neil D. Lawrence, and Kilian Q. Weinberger (Eds.). 1071–1079. http://papers.nips.cc/paper/5444-learning-neural-network-policies-with-guided-policy-search-under-unknown-dynamics

[26] Xiao Li and Calin Belta. 2019. Temporal Logic Guided Safe Reinforcement Learning Using Control Barrier Functions. *CoRR* abs/1903.09885 (2019). arXiv:1903.09885 http://arxiv.org/abs/1903.09885

[27] Timothy P. Lillicrap, Jonathan J. Hunt, Alexander Pritzel, Nicolas Heess, Tom Erez, Yuval Tassa, David Silver, and Daan Wierstra. 2016. Continuous control with deep reinforcement learning. In *4th International Conference on Learning Representations, ICLR 2016, San Juan, Puerto Rico, May 2-4, 2016, Conference Track Proceedings*, Yoshua Bengio and Yann LeCun (Eds.). http://arxiv.org/abs/1509.02971

[28] Xuankang Lin, He Zhu, Roopsha Samanta, and Suresh Jagannathan. 2019. ART: Abstraction Refinement-Guided Training for Provably Correct Neural Networks. *CoRR* abs/1907.10662 (2019). arXiv:1907.10662 http://arxiv.org/abs/1907.10662

[29] Horia Mania, Aurelia Guy, and Benjamin Recht. 2018. Simple random search of static linear policies is competitive for reinforcement learning. In *Advances in Neural Information Processing Systems 31: Annual Conference on Neural Information Processing Systems 2018, NeurIPS 2018, 3-8 December 2018, Montréal, Canada*, Samy Bengio, Hanna M. Wallach, Hugo Larochelle, Kristen Grauman, Nicolò Cesa-Bianchi, and Roman Garnett (Eds.). 1805–1814. http://papers.nips.cc/paper/7451-simple-random-search-of-static-linear-policies-is-competitive-for-reinforcement-learning

[30] Matthew Mirman, Timon Gehr, and Martin T. Vechev. 2018. Differentiable Abstract Interpretation for Provably Robust Neural Networks. In *Proceedings of the 35th International Conference on Machine Learning, ICML 2018, Stockholmsmässan, Stockholm, Sweden, July 10-15, 2018 (Proceedings of Machine Learning Research, Vol. 80)*, Jennifer G. Dy and Andreas Krause (Eds.). PMLR, 3575–3583. http://proceedings.mlr.press/v80/mirman18b.html

[31] Teodor Mihai Moldovan and Pieter Abbeel. 2012. Safe Exploration in Markov Decision Processes. In *Proceedings of the 29th International Conference on Machine Learning, ICML 2012, Edinburgh, Scotland, UK, June 26 - July 1, 2012*. icml.cc / Omnipress. http://icml.cc/2012/papers/838.pdf

[32] Adam Paszke, Sam Gross, Francisco Massa, Adam Lerer, James Bradbury, Gregory Chanan, Trevor Killeen, Zeming Lin, Natalia Gimelshein, Luca Antiga, Alban Desmaison, Andreas Köpf, Edward Yang, Zachary DeVito, Martin Raison, Alykhan Tejani, Sasank Chilamkurthy, Benoit Steiner, Lu Fang, Junjie Bai, and Soumith Chintala. 2019. PyTorch: An Imperative Style, High-Performance Deep Learning Library. In *Advances in Neural Information Processing Systems 32: Annual Conference on Neural Information Processing Systems 2019, NeurIPS 2019, 8-14 December 2019, Vancouver, BC, Canada*. 8024–8035. http://papers.nips.cc/paper/9015-pytorch-an-imperative-style-high-performance-deep-learning-library

[33] Aravind Rajeswaran, Kendall Lowrey, Emanuel Todorov, and Sham M. Kakade. 2017. Towards Generalization and Simplicity in Continuous Control. In *Advances in Neural Information Processing Systems 30: Annual Conference on Neural Information Processing Systems 2017, 4-9 December 2017, Long Beach, CA, USA*, Isabelle Guyon, Ulrike von Luxburg, Samy Bengio, Hanna M. Wallach, Rob Fergus, S. V. N. Vishwanathan, and Roman Garnett (Eds.). 6550–6561. http://papers.nips.cc/paper/7233-towards-generalization-and-simplicity-in-continuous-control

[34] Stéphane Ross, Geoffrey J. Gordon, and Drew Bagnell. 2011. A Reduction of Imitation Learning and Structured Prediction to No-Regret Online Learning. In *Proceedings of the Fourteenth International Conference on Artificial Intelligence and Statistics, AISTATS 2011, Fort Lauderdale, USA, April 11-13, 2011 (JMLR Proceedings, Vol. 15)*, Geoffrey J. Gordon, David B. Dunson, and Miroslav Dudík (Eds.). JMLR.org, 627–635. http://proceedings.mlr.press/v15/ross11a/ross11a.pdf

[35] John Schulman, Sergey Levine, Pieter Abbeel, Michael I. Jordan, and Philipp Moritz. 2015. Trust Region Policy Optimization. In *Proceedings of the 32nd International Conference on Machine Learning, ICML 2015, Lille, France, 6-11 July 2015 (JMLR Workshop and Conference Proceedings, Vol. 37)*, Francis R. Bach and David M. Blei (Eds.). JMLR.org, 1889–1897. http://proceedings.mlr.press/v37/schulman15.html

[36] Gagandeep Singh, Timon Gehr, Matthew Mirman, Markus Püschel, and Martin T. Vechev. 2018. Fast and Effective Robustness Certification. In *Advances in Neural Information Processing Systems 31: Annual Conference on Neural Information Processing Systems 2018, NeurIPS 2018, 3-8 December 2018, Montréal, Canada*, Samy Bengio, Hanna M. Wallach, Hugo Larochelle, Kristen Grauman, Nicolò Cesa-Bianchi, and Roman Garnett (Eds.). 10825–10836. http://papers.nips.cc/paper/8278-fast-and-effective-robustness-certification

[37] Gagandeep Singh, Timon Gehr, Markus Püschel, and Martin T. Vechev. 2019. An abstract domain for certifying neural networks. *Proc. ACM Program. Lang.* 3, POPL (2019), 41:1–41:30. https://doi.org/10.1145/3290354

[38] Armando Solar-Lezama. 2008. *Program synthesis by sketching*. Ph.D. Dissertation. University of California, Berkeley.

[39] Xiaowu Sun, Haitham Khedr, and Yasser Shoukry. 2019. Formal verification of neural network controlled autonomous systems. In *Proceedings of the 22nd ACM International Conference on Hybrid Systems: Computation and Control, HSCC 2019, Montreal, QC, Canada, April 16-18, 2019*, Necmiye Ozay and Pavithra Prabhakar (Eds.). ACM, 147–156. https://doi.org/10.1145/3302504.3311802

[40] Emanuel Todorov, Tom Erez, and Yuval Tassa. 2012. MuJoCo: A physics engine for model-based control.. In *IROS*. IEEE, 5026–5033. http://dblp.uni-trier.de/db/conf/iros/iros2012.html#TodorovET12

[41] Hoang-Dung Tran, Xiaodong Yang, Diego Manzanas Lopez, Patrick Musau, Luan Viet Nguyen, Weiming Xiang, Stanley Bak, and Taylor T. Johnson. 2020. NNV: The Neural Network Verification Tool for Deep Neural Networks and Learning-Enabled Cyber-Physical Systems. In *Computer Aided Verification - 32nd International Conference, CAV 2020, Los Angeles, CA, USA, July 21-24, 2020, Proceedings, Part I (Lecture Notes in Computer Science, Vol. 12224)*, Shuvendu K. Lahiri and Chao Wang (Eds.). Springer, 3–17. https://doi.org/10.1007/978-3-030-53288-8_1

[42] Matteo Turchetta, Felix Berkenkamp, and Andreas Krause. 2016. Safe Exploration in Finite Markov Decision Processes with Gaussian Processes. In *Advances in Neural Information Processing Systems 29: Annual Conference on Neural Information Processing Systems 2016, December 5-10, 2016, Barcelona, Spain*, Daniel D. Lee, Masashi Sugiyama, Ulrike von Luxburg, Isabelle Guyon, and Roman Garnett (Eds.). 4305–4313. http://papers.nips.cc/paper/6358-safe-exploration-in-finite-markov-decision-processes-with-gaussian-processes

[43] Jonathan Uesato, Ananya Kumar, Csaba Szepesvári, Tom Erez, Avraham Ruderman, Keith Anderson, Krishnamurthy (Dj) Dvijotham, Nicolas Heess, and Pushmeet Kohli. 2019. Rigorous Agent Evaluation: An Adversarial Approach to Uncover Catastrophic Failures. In *7th International Conference on Learning Representations, ICLR 2019, New Orleans, LA, USA, May 6-9, 2019*. OpenReview.net. https://openreview.net/forum?id=B1xhQhRcK7

[44] Abhinav Verma, Vijayaraghavan Murali, Rishabh Singh, Pushmeet Kohli, and Swarat Chaudhuri. 2018. Programmatically Interpretable Reinforcement Learning. In *Proceedings of the 35th International Conference on Machine Learning, ICML 2018, Stockholmsmässan, Stockholm, Sweden, July 10-15, 2018 (Proceedings of Machine Learning Research,*

Vol. 80), Jennifer G. Dy and Andreas Krause (Eds.). PMLR, 5052–5061. http://proceedings.mlr.press/v80/verma18a.html

[45] Shiqi Wang, Yizheng Chen, Ahmed Abdou, and Suman Jana. 2018. MixTrain: Scalable Training of Formally Robust Neural Networks. *CoRR* abs/1811.02625 (2018). http://arxiv.org/abs/1811.02625

[46] Shiqi Wang, Kexin Pei, Justin Whitehouse, Junfeng Yang, and Suman Jana. 2018. Formal Security Analysis of Neural Networks using Symbolic Intervals. In *27th USENIX Security Symposium, USENIX Security 2018, Baltimore, MD, USA, August 15-17, 2018*, William Enck and Adrienne Porter Felt (Eds.). USENIX Association, 1599–1614. https://www.usenix.org/conference/usenixsecurity18/presentation/wang-shiqi

[47] Tsui-Wei Weng, Huan Zhang, Hongge Chen, Zhao Song, Cho-Jui Hsieh, Luca Daniel, Duane S. Boning, and Inderjit S. Dhillon. 2018. Towards Fast Computation of Certified Robustness for ReLU Networks. In *Proceedings of the 35th International Conference on Machine Learning, ICML 2018, Stockholmsmässan, Stockholm, Sweden, July 10-15, 2018 (Proceedings of Machine Learning Research, Vol. 80)*, Jennifer G. Dy and Andreas Krause (Eds.). PMLR, 5273–5282. http://proceedings.mlr.press/v80/weng18a.html

[48] P. J. Werbos. 1990. Backpropagation through time: what it does and how to do it. *Proc. IEEE* 78, 10 (1990), 1550–1560. https://doi.org/10.1109/5.58337

[49] Eric Wong and J. Zico Kolter. 2018. Provable Defenses against Adversarial Examples via the Convex Outer Adversarial Polytope. In *Proceedings of the 35th International Conference on Machine Learning, ICML 2018, Stockholmsmässan, Stockholm, Sweden, July 10-15, 2018 (Proceedings of Machine Learning Research, Vol. 80)*, Jennifer G. Dy and Andreas Krause (Eds.). PMLR, 5283–5292. http://proceedings.mlr.press/v80/wong18a.html

[50] Mojtaba Zarei, Yu Wang, and Miroslav Pajic. 2020. Statistical verification of learning-based cyber-physical systems. In *HSCC '20: 23rd ACM International Conference on Hybrid Systems: Computation and Control, Sydney, New South Wales, Australia, April 21-24, 2020*, Aaron D. Ames, Sanjit A. Seshia, and Jyotirmoy Deshmukh (Eds.). ACM, 12:1–12:7. https://doi.org/10.1145/3365365.3382209

[51] Huan Zhang, Hongge Chen, Chaowei Xiao, Sven Gowal, Robert Stanforth, Bo Li, Duane S. Boning, and Cho-Jui Hsieh. 2020. Towards Stable and Efficient Training of Verifiably Robust Neural Networks. In *8th International Conference on Learning Representations, ICLR 2020, Addis Ababa, Ethiopia, April 26-30, 2020*. OpenReview.net. https://openreview.net/forum?id=Skxuk1rFwB

[52] He Zhu, Zikang Xiong, Stephen Magill, and Suresh Jagannathan. 2019. An inductive synthesis framework for verifiable reinforcement learning. In *Proceedings of the 40th ACM SIGPLAN Conference on Programming Language Design and Implementation, PLDI 2019, Phoenix, AZ, USA, June 22-26, 2019*, Kathryn S. McKinley and Kathleen Fisher (Eds.). ACM, 686–701. https://doi.org/10.1145/3314221.3314638